the plant journal

SEB Society for Experimental Biology

The Plant Journal (2013) **74,** 678–689 doi: 10.1111/tpj.12156

A variant of LEAFY reveals its capacity to stimulate meristem development by inducing *RAX1*

Hicham Chahtane[1,2,3,4], Gilles Vachon[1,2,3,4], Marie Le Masson[1,2,3,4], Emmanuel Thévenon[1,2,3,4], Sophie Périgon[1,2,3,4,†], Nela Mihajlovic[5], Anna Kalinina[5], Robin Michard[1,2,3,4], Edwige Moyroud[1,2,3,4,‡], Marie Monniaux[1,2,3,4], Camille Sayou[1,2,3,4], Vojislava Grbic[5], Francois Parcy[1,2,3,4,*,§] and Gabrielle Tichtinsky[1,2,3,4]

[1]*Laboratoire Physiologie Cellulaire et Végétale, CEA (Commissariat à l'Energie Atomique et aux Energies Alternatives), iRTSV (Institut de Recherches en Technologies et Sciences pour le Vivant), Grenoble F-38054, France,*

[2]*Centre National de la Recherche Scientifique, UMR5168, Grenoble F-38054, France,*

[3]*Université Joseph Fourier-Grenoble I, UMR5168, Grenoble F-38041, France,*

[4]*Institut National de la Recherche Agronomique, USC1359, Grenoble F-38054, France, and*

[5]*Department of Biology, University of Western Ontario, London, ON N6A 5B8, Canada*

Received 28 November 2012; revised 13 February 2013; accepted 19 February 2013; published online 27 February 2013.

*For correspondence (e-mail francois.parcy@cea.fr).

[†]Present address: Laboratoire d'Ecologie Alpine, Centre National de la Recherche Scientifique, UMR 5553, Grenoble F-38041, France.

[‡]Present address: Department of Plant Sciences, University of Cambridge, Downing Street, Cambridge CB2 3EA, UK.

[§]Present address: Centre for Molecular Medicine and Therapeutics, Child and Family Research Institute, University of British Columbia, Vancouver, BC V5Z 4H4, Canada.

SUMMARY

In indeterminate inflorescences, floral meristems develop on the flanks of the shoot apical meristem, at positions determined by auxin maxima. The floral identity of these meristems is conferred by a handful of genes called floral meristem identity genes, among which the LEAFY (LFY) transcription factor plays a prominent role. However, the molecular mechanism controlling the early emergence of floral meristems remains unknown. A body of evidence indicates that LFY may contribute to this developmental shift, but a direct effect of LFY on meristem emergence has not been demonstrated. We have generated a *LFY* allele with reduced floral function and revealed its ability to stimulate axillary meristem growth. This role is barely detectable in the *lfy* single mutant but becomes obvious in several double mutant backgrounds and plants ectopically expressing LFY. We show that this role requires the ability of LFY to bind DNA, and is mediated by direct induction of *REGULATOR OF AXILLARY MERISTEMS1* (*RAX*1) by LFY. We propose that this function unifies the diverse roles described for LFY in multiple angiosperm species, ranging from monocot inflorescence identity to legume leaf development, and that it probably pre-dates the origin of angiosperms.

Keywords: meristem development, flower, LEAFY, *RAX1*, *Arabidopsis thaliana*.

INTRODUCTION

In plants bearing raceme inflorescences such as *Arabidopsis thaliana*, flowers arise on the flanks of the shoot apical meristem. They initially emerge as small groups of cells that acquire first meristematic identity and then floral identity, to eventually produce flower buds. Meristematic identity is first evident in the shape and organization of this domed group of dividing cells (stages 1–2), and later in the molecular markers that they express, such as *CLAVATA3* (*CLV3*), *WUSCHEL* (*WUS*) and *UNUSUAL FLORAL ORGANS* (*UFO*) (stages 2–3). Floral meristem identity genes determine floral identity (Liu *et al.*, 2009; Wagner, 2009; Irish, 2010; Moyroud *et al.*, 2010; Pose *et al.*, 2012). This class includes *LEAFY* (*LFY*) and *APETALA1* (*AP1*), which control the development of flowers and their patterning through induction of organ identity genes such as *AGAMOUS* (*AG*) and *APETALA3* (*AP3*). *LFY* and *AP1* act very early in meristem development (stages 0–1) and share many direct target genes (Kaufmann *et al.*, 2010; Moyroud *et al.*, 2011; Winter *et al.*, 2011). Although determination of floral meristem identity has been intensively studied and is well understood, how the initial group of cells acquires its meristematic identity remained unknown. It is known that auxin maxima determine where floral meristems arise (Kuhlemeier, 2007; Vernoux *et al.*, 2010), but the link between auxin signaling and induction of meristematic features has not yet been fully established.

Several observations indicate that LFY is a possible candidate to mediate this action. First, *LFY* expression is controlled by auxin as shown in *pin* mutants (Vernoux *et al.*, 2000; Lebedeva *et al.*, 2005; Blazquez *et al.*, 2006). Second, scattered data suggest that LFY may play a role in conferring meristematic identity to the floral meristem (Moyroud *et al.*, 2009, 2010). Finally, LFY is able to induce meristematic identity in other developmental contexts, for instance to create compound leaves in some legumes, tillers in rice (*Oryza sativa*), or complex inflorescences in rice and maize (*Zea mays*) (Moyroud *et al.*, 2009, 2010). LFY may thus provide the link between auxin signaling and meristematic growth. However, LFY is not required for meristem development *per se*: in the *lfy* single mutant, flowers are replaced by cauline leaves that bear a meristematic structure in their axil. This structure gives rise to shoots or shoot/flower intermediates. It is only when the *lfy* mutation is combined with defects in genes such as *PINOID* (*PID*) (Ezhova *et al.*, 2000), *CLV1* (Clark *et al.*, 1993), *FILAMENTOUS FLOWERS* (*FIL*) (Chen *et al.*, 1999; Sawa *et al.*, 1999a), *ENHANCED RESPONSE TO ABA* (*ERA*) (Running *et al.*, 1998; Yalovsky *et al.*, 2000), *FUSED FLORAL ORGANS* (*FFO*) (Levin *et al.*, 1998), *FLOWERING LOCUS T* (*FT*), *FWA* (Ruiz-Garcia *et al.*, 1997) or *BLADE ON PETIOLE1/2* (*BOP1/2*) (Norberg *et al.*, 2005) that leaves lacking axillary meristems develop at some positions on the inflorescence (referred to as empty cauline leaves).

Here we provide direct evidence in *A. thaliana* that LFY has the capacity to trigger meristem growth. We obtained this evidence by altering the properties of the LFY protein. LFY has two conserved functional domains: an N-terminal dimerization domain and a C-terminal DNA-binding domain (DBD) (Hamès *et al.*, 2008; Siriwardana and Lamb, 2012). The DBD dimerizes upon DNA binding. Taking advantage of its crystallographic structure, we engineered a form of the LFY DBD (called LFY_{HARA}) that has a compromised dimerization interface. When expressed in plants, this allele shows reduced floral function, thereby revealing the ability of LFY to stimulate the emergence of meristems.

RESULTS

The HARA mutation reduces the affinity of LFY for DNA without affecting its sequence specificity

Two amino acid residues (H387 and R390) involved in dimerization of the LFY DBD (Figure 1a) have been identified previously, but their importance was only established *in vitro* using the isolated LFY DBD (Hamès *et al.*, 2008); their role within the context of a full-length LFY protein, which contains the conserved N-terminal dimerization domain (Siriwardana and Lamb, 2012), has not been determined. We thus analyzed the properties of the near full-length LFY_{HARA}(Δ40) protein (see Experimental procedures), in which both the H387 and R390 residues are mutated to alanine, thereby suppressing the hydrogen bonds between the DBD monomers (Figure 1a). Using EMSA analysis (Figure 1b), we found that LFY_{HARA}(Δ40) binds *AP1*bs1, a binding site present in the *AP1* promoter (Benlloch *et al.*, 2011), but with weaker affinity than wild-type LFY(Δ40). This result confirms the importance of

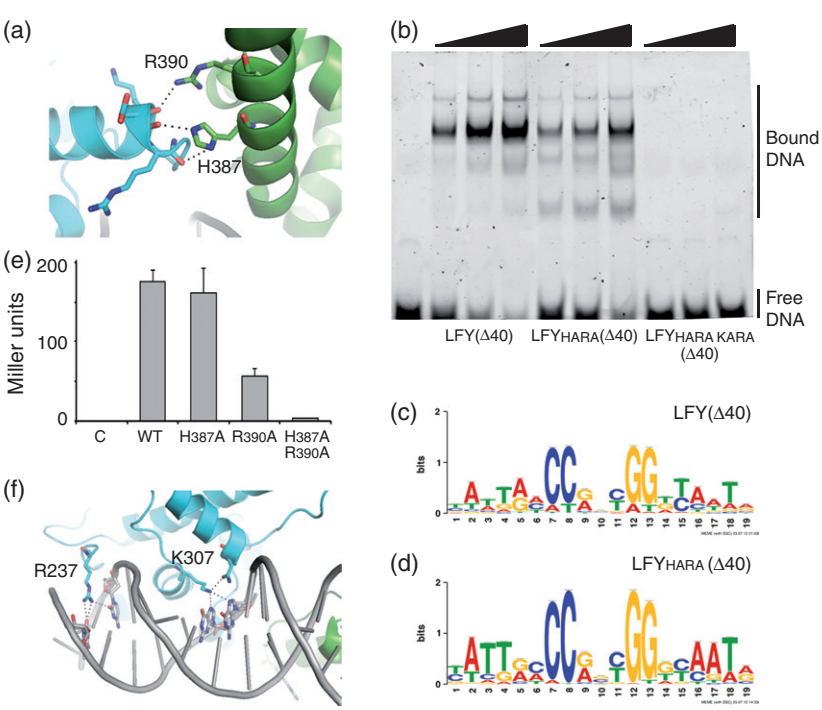

Figure 1. Biochemical characterization of the LFY_{HARA} and $LFY_{HARAKARA}$ proteins.
(a) Details of the structure of a LFY DBD dimer (Hamès *et al.*, 2008) showing the hydrogen bonds (dotted lines) between monomers (shown in blue and green) involving His387 (H387) and Arg390 (R390).
(b) Electrophoretic mobility shift assay (EMSA) using the same increasing quantities of LFY (Δ40), LFY_{HARA}(Δ40) and $LFY_{HARAKARA}$(Δ40) mixed with the *AP1*bs1 binding site (Benlloch *et al.*, 2011).
(c, d) Logos illustrating position-specific scoring matrixes obtained by high-throughput SELEX experiments performed with LFY(Δ40) (c) and LFY_{HARA}(Δ40) (d).
(e) Yeast one-hybrid assay. LFY proteins were fused to the viral VP16 activation domain. Their ability to bind the regulatory sequences of *AG* was followed using the activity of the reporter gene *AG:LACZ* (β-galactosidase activity). C: Control (LFY unfused to VP16); WT: wild –type LFY-VP16; H387A: LFY_{HA}-VP16; R390A: LFY_{RA}-VP16; H387A R390A: LFY_{HARA}-VP16. Error bars indicate the standard error of the mean (n = 10).
(f) Detail of the LFY/DNA interaction (Hamès *et al.*, 2008) showing hydrogen bonds (dotted lines) between Lys307 (K307) and Arg237 (R237) and the DNA bases.

contacts between the DBDs even in the presence of the N-terminal dimerization domain. To test whether the HARA mutations affect LFY DNA-binding specificity, we performed a high-throughput Systematic evolution of ligands by exponential enrichment (SELEX) experiment (Zhao *et al.*, 2009). The resulting logo, representing the DNA-binding preferences of $LFY_{HARA}(\Delta 40)$ (Figure 1c,d), was found to be extremely similar to the one obtained for LFY(Δ40), indicating that the HARA mutations do not greatly affect LFY DNA-binding specificity. We also tested the importance of LFY DBD dimerization in a yeast one-hybrid assay. Because LFY displays no transcriptional activity in yeast, full-length LFY and LFY_{HARA} proteins were fused to the VP16 transcriptional activation domain (Parcy *et al.*, 1998; Lohmann *et al.*, 2001), and their activity were tested using *AGAMOUS* (*AG*) regulatory sequences cloned upstream of the *lacZ* reporter gene. As shown in Figure 1(e), the activity of LFY_{HARA} was dramatically reduced compared to LFY, showing that HARA mutations strongly weaken the ability of LFY to bind to *AG* regulatory sequences.

LFY_{HARA} is impaired in its floral meristem identity function

We next tested the functional relevance of LFY DBD dimerization in plants. *LFY* and LFY_{HARA} coding sequences were placed under the control of the *LFY* endogenous promoter (*ProLFY*) in a *lfy-12* null mutant background. In 9 of 10 $lfy\text{-}12^{-/-}$ primary transformants, the *ProLFY:LFY* construct rescued the *lfy* mutant phenotype almost fully: flowers were present all along the main inflorescence and most displayed a wild-type appearance and correctly arranged floral organs (Figure 2c,e and Table S1). Although the $ProLFY:LFY_{HARA}$ transgene also induced flower formation in eight of nine $lfy\text{-}12^{-/-}$ primary transformants (Figure 2d and Table S1), flower development was systematically abnormal compared to wild-type or *ProLFY:LFY* plants. Petals and stamens were either missing or distorted, frequently resulting in sterile flowers (Figure 2e and Table S1). Occasionally, the shoot apical meristem produced a few fertile flowers on the lower positions of the inflorescence, and shoot-like structures at higher positions on the stem (Figure S1), revealing the weakened ability of LFY_{HARA} to trigger flower development. These results indicate that the capacity of LFY to control flower formation is reduced (but not abolished) when the two amino acids, H387 and R390, are mutated.

LFY_{HARA} over-expression triggers precocious meristem development in the axil of rosette leaves

Upon floral transition, several partially independent pathways converge to build flowers at the inflorescence meristem (Fornara *et al.*, 2010). To assess the function of LFY_{HARA} independently of these other pathways, we ectopically expressed *LFY* and LFY_{HARA} under control of the 35S CaMV promoter (*Pro35S*). Under long-day conditions, 5-week-old wild-type plants displayed no visible axillary structures at the base of rosette leaves (Figure 2f). As previously described (Weigel and Nilsson, 1995), over-expression of the wild-type *LFY* cDNA induced formation of ectopic flowers in the axils of rosette and cauline leaves, as well as termination of the main shoot in a solitary flower (Figure 2g). In contrast, $Pro35S:LFY_{HARA}$ plants displayed no or very few ectopic flowers; instead, they showed precocious emergence of axillary shoots compared to wild-type plants (Figure 2h and Table S2). This effect was even more evident under short-day conditions, where $Pro35S:LFY_{HARA}$ plants became so bushy that the primary shoot was indistinguishable from the numerous secondary inflorescences (Figure 2i,j).

The growth of rosette axillary shoots in $Pro35S:LFY_{HARA}$ plants may be due to accelerated development of their meristems or insensitivity to the apical dominance imposed by the shoot apical meristem. In order to distinguish between these possibilities, we performed a decapitation experiment: we pruned the apical meristem to reduce apical dominance and counted visible axillary shoots after 10 days. In wild-type and *lfy-12* mutant plants, decapitation resulted in a two- to threefold increased proportion of rosette leaves bearing visible shoots at their axil (Figure 2k). $Pro35S:LFY_{HARA}$ plants also responded to decapitation to a similar extent, despite the fact they already displayed a high number of axillary shoots before decapitation (Figure 2k). This result shows that $Pro35S:LFY_{HARA}$ plants are still sensitive to apical dominance. Next we studied the time course of axillary meristem initiation. To do this, we monitored the expression of the *CLV3:GUS* meristematic marker (Brand *et al.*, 2002) during seedling development (Figure 3a–c). We found that, on average, the *CLV3:GUS* signal appeared 3.5 days earlier at the axil of rosette leaves in $Pro35S:LFY_{HARA}$ seedlings than in wild-type seedlings (Figure 3a). In representative 16-day-old wild-type seedlings, only the apical meristem was stained (Figure 3b), whereas in $Pro35S:LFY_{HARA}$ seedlings, several axillary meristems also showed *CLV3:GUS* expression (Figure 3c).

Wild-type *LFY* over-expression also accelerates axillary meristem development

To determine whether the wild-type *LFY* gene (and not only the LFY_{HARA} allele) influences rosette axillary meristem development, we analyzed *Pro35S:LFY* plants. We used short-day conditions to delay precocious flowering, and included *Pro35S:AP1* plants, which share many features with *Pro35S:LFY* plants, such as conversion of axillary meristems into flowers (Mandel and Yanofsky, 1995). To determine the developmental rate of meristem initiation and growth at the axil of rosette leaves, we scored the developmental stage of the axillary meristem at each inter-

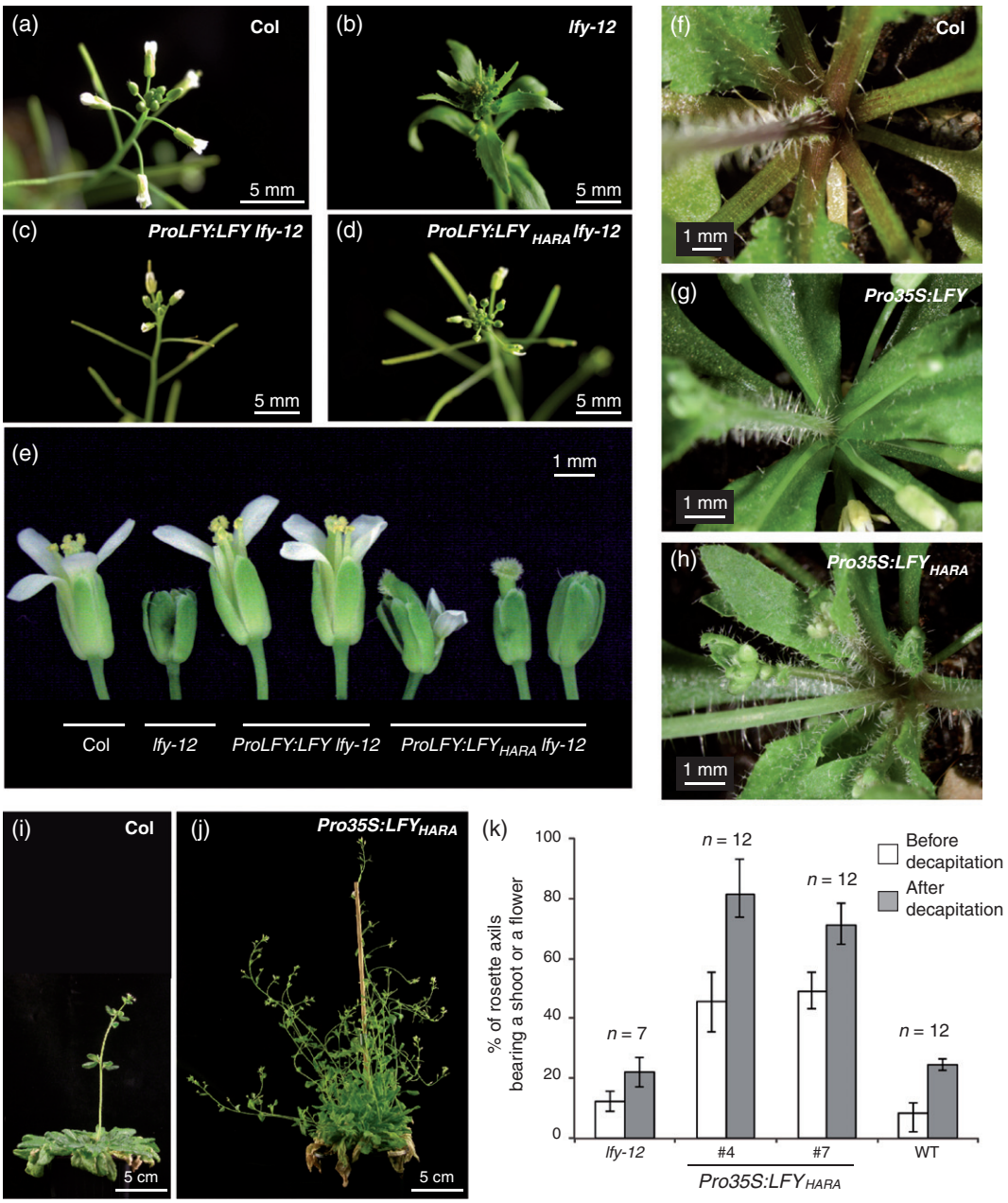

Figure 2. *ProLFY:LFY* and *Pro35S:LFY* transgenic Arabidopsis.
(a–d) Inflorescences of wild-type Col-0 (a), *lfy-12* mutant (b), *ProLFY:LFY lfy-12* (c) and *ProLFY:LFY*$_{HARA}$ *lfy-12* (d) plants.
(e) Corresponding floral phenotypes. Some floral organs of *ProLFY:LFY lfy-12* flowers are distorted. Petal and stamen number are frequently reduced in the flowers of *ProLFY:LFY*$_{HARA}$ *lfy-12* plants.
(f–h) Close-up view of the rosette of 5-week-old wild-type and *Pro35S:LFY* plants. The axils of wild-type plants do not show any macroscopic structures (f), whereas flowers and shoots developed at the axils of *Pro35S:LFY* (g) or *Pro35S:LFY*$_{HARA}$ (h) rosette leaves, respectively.
(i, j) Wild-type plant (i) and *Pro35S: LFY*$_{HARA}$ plant (j) cultivated for 2 months under short-day conditions.
(k) Percentage of rosette leaves bearing a flower or a shoot at their axil just before decapitation and 10 days after decapitation of the primary inflorescence. The number of individuals tested is indicated for each genotype, i.e. wild-type plants, *lfy-12* mutants and two independent homozygous *Pro35S:LFY*$_{HARA}$ lines (#4 and #7). Error bars represent 95% confidence intervals.

node as described previously (Stirnberg *et al.*, 2002). Stage 1 is when a group of densely stained cells become visible at the leaf axil; stage 2 is when meristematic dome forms at the leaf axil; stage 3 is when axillary meristems commence primordial initiation (Figure 3d–f). Plastochron formation was used as the developmental time unit. Stage 1 was observed after 17 plastochrons in Col plants, but only after nine plastochrons (on average) in *Pro35S:LFY* plants. The difference between *Pro35S:LFY* and Col is even more striking for progression to stages 2 and 3. Axillary meris-

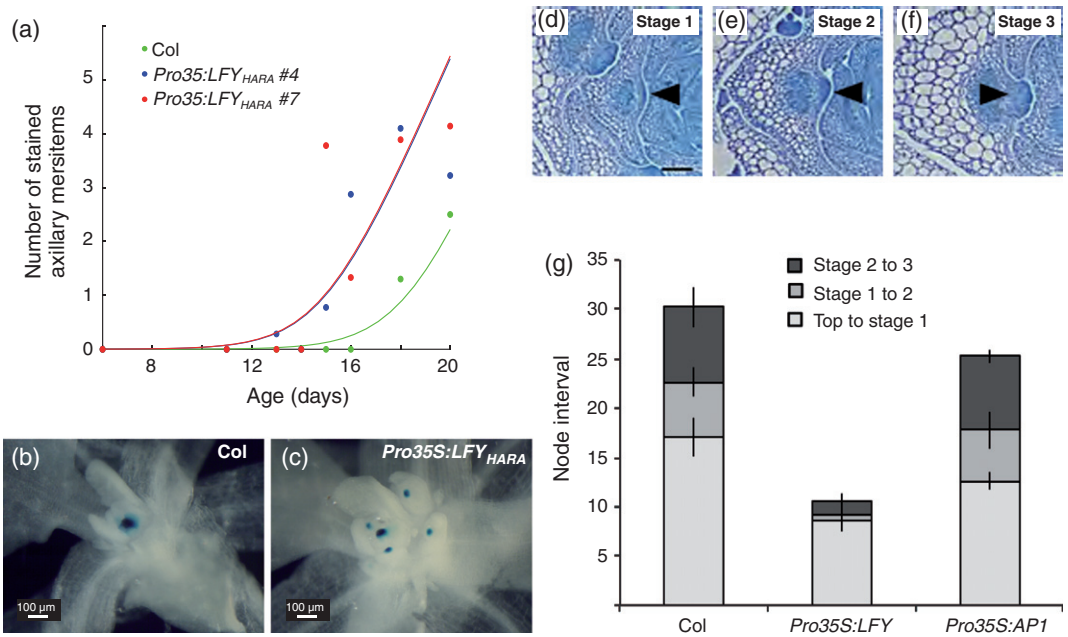

Figure 3. Characterization of axillary meristem development in *Pro35S:LFY*, *Pro35S:LFY$_{HARA}$* and *Pro35S:AP1* plants.
(a–c) *CLV3:GUS* expression in *Pro35S:LFY$_{HARA}$* and wild-type seedlings grown under long-day conditions. (a) Kinetics of *CLV3:GUS* activity in axillary meristems during seedling development. The mean number of stained axillary meristems is indicated as green, blue and red circles for wild-type plants and *Pro35S:LFY$_{HARA}$* lines (#4 and #7), respectively (n = 5–12). A mathematical model was constructed to describe these data (see Experimental procedures). The corresponding green, blue and red fitting curves are shown. According to this model, the plants entered the phase of axillary meristem production at day 18.3 (17.2–19.5) for wild-type plants versus day 15.0 (14.2–15.8) and 14.9 (14.1–16.8) for *Pro35S:LFY$_{HARA}$* lines #4 and #7, respectively (95% confidence intervals in parentheses). Representative 16-day-old wild-type (b) and *Pro35S:LFY$_{HARA}$* (c) seedlings are shown.
(d–g) Development of the axillary meristem in *Pro35S:LFY*, *Pro35S:AP1* and wild-type (Col) plants grown under short-day conditions. (d–f) Transverse sections of individual shoots illustrating the stages of axillary meristem development (arrowheads) according to Stirnberg *et al.* (2002). Scale bar = 20 µm. (g) Mean number of node intervals, or plastochrons, between the shoot apex and the first stage 1 axillary meristem (top to stage 1), between the first stage 1 and the first stage 2 axillary meristems (stage 1 to 2), and between the first stage 2 and the first stage 3 axillary meristems (stage 2 to 3). Error bars indicate the standard error of the mean (n = 3–12).

tems at stage 2 were frequently absent in *Pro35S:LFY* plants, and axillary meristems at stages 1 and 3 were seen in adjacent plastochrons. This contrasts with the slower development of axillary meristems in Col and *Pro35S:AP1* plants, where it took over five plastochrons (on average) to progress from stage 1 to stage 2, and 7.5 additional plastochrons to reach stage 3 (Figure 3g). This experiment showed that axillary meristems develop faster in *Pro35S:LFY* plants than in wild-type or *Pro35S:AP1* plants. Given that the plastochron rate is not slower in *35S:LFY* plants than in wild-type plants (Figure S2), this clearly demonstrates that LFY accelerates axillary meristem development. A further inspection of *Pro35S:LFY* plants revealed the occasional presence of meristems in the axils of cotyledons (Table S3), a structure commonly observed in the *Pro35S:LFY$_{HARA}$* plants (Figure S3) or in mutants such as *branched1* (Aguilar-Martinez *et al.*, 2007), but extremely rare in wild-type plants.

The meristematic function of LEAFY requires DNA binding

The experiments described above suggest that LFY may have two distinct and sequential functions: first, LFY may trigger the development of meristems, and then convert them into flowers. LFY DNA binding is essential for the later function, but whether it is required for the first role has never been tested. To answer this question, we took advantage of the crystallographic structure of LFY DBD (Hamès *et al.*, 2008) and specifically disrupted the interaction of LFY with DNA: in addition to H387 and R390 involved in dimerization, we mutated the two key amino acids (K307 and R237), which contact DNA bases directly, into alanines (Figure 1f). We confirmed *in vitro* that the resulting LFY$_{HARAKARA}$ mutant protein had lost its ability to specifically bind DNA sequences (Figure 1b). Next, we ectopically expressed *LFY$_{HARAKARA}$* in transgenic Arabidopsis: these plants were indistinguishable from wild-type plants (Table S2), demonstrating that, as for the floral function, the meristematic function of LFY requires LFY DNA binding. This result suggests that LFY fulfils this function by directly regulating downstream target genes.

The LFY meristematic function involves up-regulation of *RAX1*

We next assessed through which pathway LFY mediates this function. Among genes bound by LFY in ChIP experiments (Moyroud *et al.*, 2011; Winter *et al.*, 2011), we found

several that are known to contribute to meristem or axillary meristem development: *REGULATOR OF AXILLARY MERISTEMS 1* (*RAX1*) (Keller *et al.*, 2006; Muller *et al.*, 2006), participating in axillary meristem development, *TERMINAL EAR LIKE2* (*TEL2*) (Anderson *et al.*, 2004), which is probably involved in meristem maintenance, *ARABIDOPSIS RESPONSE REGULATOR* (*ARR7*), which is involved in cytokinin signaling (Lee *et al.*, 2007), and *GROWTH REGULATOR FACTOR5* (*GRF5*) (Kim *et al.*, 2003; Horiguchi *et al.*, 2005). To determine whether these genes are genuinely regulated by LFY (and not just bound), we analyzed their transcript levels in various tissues and genetic backgrounds where LFY expression or activity was modified relative to wild-type plants. We used inflorescences from *lfy-12* and *ProLFY:LFY-VP16* plants (Parcy *et al.*, 1998) to assess regulation in floral tissues. We also used young seedlings of *Pro35S:LFY* transgenic plants to monitor gene expression in a context that minimizes the influence of inflorescence-specific redundant pathways. In this assay, known LFY direct target genes such as *AP1*, an induced target, or *TERMINAL FLOWER1* (*TFL1*), a repressed one, served as positive controls (Figure 4a) and behaved as expected from the published data (Parcy *et al.*, 1998, 2002; Ratcliffe *et al.*, 1999). We found that *RAX1* and *TEL2* were up-regulated in *ProLFY:LFY-VP16* and *Pro35S:LFY*, showing that LFY induces expression of these two genes in both floral and seedling tissues. *ARR7* was up-regulated in all three backgrounds (seedlings of *Pro35S:LFY* and inflorescences of *ProLFY:LFY-VP16* and *lfy-12*), suggesting that it is regulated by LFY (repressed in inflorescence tissues and induced in seedlings). However, *GRF5* was not affected in any of the three genetic backgrounds, despite strong binding by LFY. Among these candidates, *RAX1* was particularly interesting for several reasons: (i) the *RAX1* locus is bound by LFY in three regions (promoter, coding sequence and 3′ untranslated region) in both *Pro35S:LFY* seedling

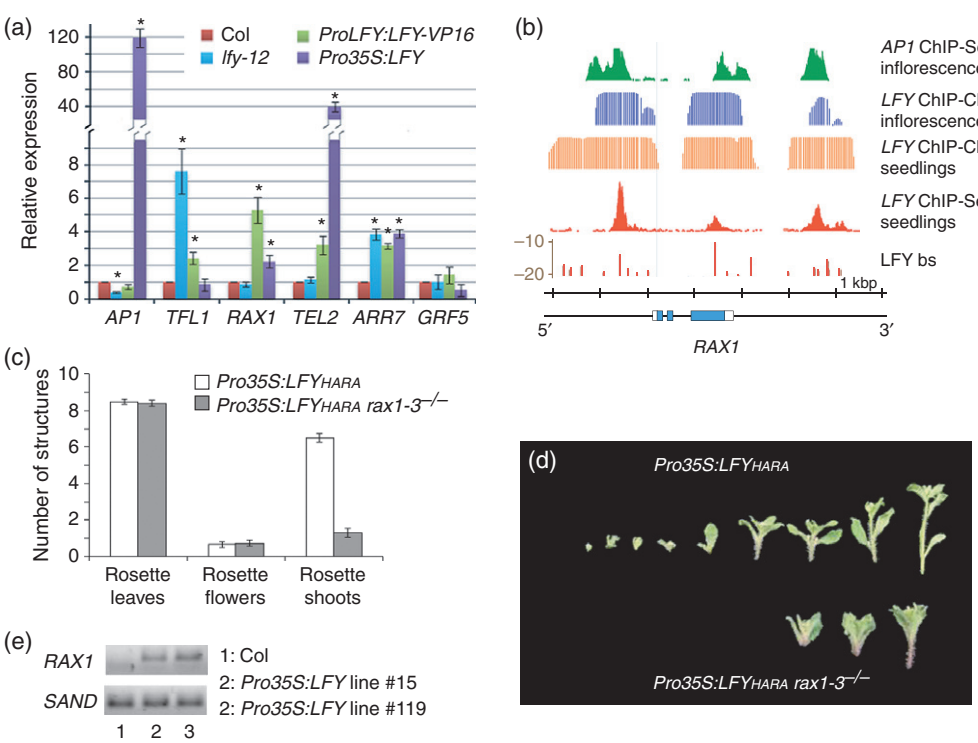

Figure 4. Identification of *RAX1* as a LFY target involved in the stimulation of the axillary meristem in *Pro35S:LFY*$_{HARA}$ plants.
(a) Expression of *AP1*, *TFL1*, *RAX1*, *TEL2*, *ARR7* and *GRF5* in wild-type, *lfy-12* mutant and *ProLFY:LFY-VP16* inflorescences, and in *Pro35S:LFY* and wild-type whole seedlings. Expression relative to wild-type is shown. Error bars indicate standard errors, and asterisks indicate statistically significant differences compared with wild-type (*P* value < 0.05) according to a randomization test (Pfaffl *et al.*, 2002).
(b) LFY and AP1 binding profiles at the *RAX1* locus. Coding and untranslated regions of the *RAX1* gene are shown as blue or white boxes, respectively. ChIP-Seq read coverage for LFY (Moyroud *et al.*, 2011) and AP1 (Kaufmann *et al.*, 2010) is shown in red and green, respectively, and ChIP/Chip data for LFY binding in inflorescences and seedlings (Winter *et al.*, 2011) are indicated in blue and orange, respectively. The LFY-binding sites (LFY bs) predicted by the LFY binding model (Moyroud *et al.*, 2011) are indicated as red bars (for scores above -20). The figure was created using the Integrated Genome Browser (Nicol *et al.*, 2009).
(c, d) A mutation in the *RAX1* gene partially reduces the number of precocious axillary structures in *Pro35S:LFY*$_{HARA}$. (c) Rosette axillary structures of *Pro35S:LFY*$_{HARA}$ plants (n = 35) and *Pro35S:LFY*$_{HARA}$ *rax1-3*$^{-/-}$ plants (n = 38). Errors bars indicate standard errors of the mean. (d) Representative *Pro35S:LFY*$_{HARA}$ and *Pro35S:LFY*$_{HARA}$ *rax1-3*$^{-/-}$ rosettes were dissected to show all axillary structures growing at the base of the rosette leaves.
(e) RT-PCR analysis of *RAX1* expression in rosette leaves of 1-month-old wild-type and *Pro35S:LFY* plants grown under long-day conditions. The *SAND* gene (At2g28390) was used as a constitutive control.

and wild-type inflorescence samples (Figure 4b) (Moyroud *et al.*, 2011; Winter *et al.*, 2011), (ii) the spatio-temporal expression pattern of *RAX1* in floral meristems correlates with *LFY* expression (Keller *et al.*, 2006; Muller *et al.*, 2006), (iii) *RAX1* is required for the emergence of axillary meristems in various conditions and genetic backgrounds (Keller *et al.*, 2006; Muller *et al.*, 2006; Yang *et al.*, 2012), and (iv) *RAX1* up-regulation in isolated *Pro35S:LFY* leaves (Figure 4e) indicates that LFY is sufficient for this induction: this regulation does not require any additional flower-specific co-factor and is direct enough to occur independently of meristem development. To determine whether *RAX1* contributes to meristem stimulation in *Pro35S:LFY$_{HARA}$* plants, we characterized *Pro35S:LFY$_{HARA}$ rax1-3* plants. Under long-day conditions, the number of shoots emerging from *rax1-3 Pro35S:LFY$_{HARA}$* rosette leaves was markedly decreased compared to *Pro35S:LFY$_{HARA}$* plants (Figure 4c, d), showing that LFY induces the formation and growth of axillary meristems at least in part through induction of the *RAX1* gene.

DISCUSSION

LFY promotes the development of axillary meristems

LEAFY is a prominent floral meristem identity gene. It is highly expressed in the youngest incipient floral primordium to which it confers a floral fate. How meristems are turned into flowers is relatively well understood, but the molecular mechanism controlling their early emergence on the flanks of the shoot apical meristem has remained more elusive.

In this paper, we combine a variety of approaches to demonstrate that LFY is able to stimulate the growth of axillary meristems. We took advantage of knowledge of the LFY DBD 3D structure to modify its properties in a subtle and precise manner. By altering the capacity of the LFY DBD to dimerize on DNA, we engineered a modified version, LFY$_{HARA}$, that partially fulfils the LFY floral function, revealing the ability of LFY to stimulate axillary bud outgrowth. This property is obvious in plants ectopically expressing LFY$_{HARA}$: their architecture is profoundly altered (particularly under short-day conditions), and the *CLV3* meristematic marker is precociously expressed in the leaf axils.

Various lines of evidence demonstrate that this property is a native characteristic of wild-type LFY rather than a neomorphic feature of the LFY$_{HARA}$ allele. First, the accelerated meristem development was also observed in plants ectopically expressing the wild-type *LFY* gene. These plants sometimes develop meristems in the axil of the cotyledons, a feature that is not present in the wild-type plants. Second, we established that LFY$_{HARA}$ not only binds to the *AP1*bs1 sequence in EMSA, but to the same set of DNA sequences as LFY in high-throughput SELEX. Third, we showed that a LFY$_{HARA}$ version that does not bind DNA (LFY$_{HARAKARA}$) loses its capacity to stimulate meristem growth. It is therefore likely that LFY$_{HARA}$ acts by binding to genuine LFY targets.

LFY stimulates meristem growth through induction of *RAX1*

Our data indicate that the *RAX1* gene is an important direct LFY target that is required for stimulation of axillary meristem growth. Indeed, *RAX1* is strongly bound by LFY in ChIP experiments (both in *Pro35S:LFY* seedlings and wild-type inflorescences) (Moyroud *et al.*, 2011; Winter *et al.*, 2011), and its transcript level is increased in whole seedlings or isolated leaves of *Pro35S:LFY* plants and in *Pro-LFY:LFY-VP16* inflorescences. Moreover, the *rax1* mutation reduces the emergence of axillary shoots in *Pro35S:LFY$_{HARA}$* plants, demonstrating that LFY induces the growth of axillary shoots through activation of *RAX1*.

LFY meristematic function is cryptic but important during flower meristem development

The *lfy* mutation compromises the emergence of a wild-type floral meristem but does not lead to a naked pin-like shoot because leaf primordia with associated axillary meristems grow instead of flowers. Similarly, during plant vegetative growth, axillary meristems emerge in the absence of *LFY* expression: LFY is therefore not required for meristem development on the flanks of the shoot apical meristem as other pathways exist that also drive this process. This redundancy may explain why the role of LFY in the emergence of floral meristems has remained unnoticed. However, when the *lfy* mutation is combined with defects in other genes, the importance of *LFY* in this process becomes clear. *FIL* and *CLV1* are two genes that act during floral meristem development (Clark *et al.*, 1993; Chen *et al.*, 1999; Sawa *et al.*, 1999a,b). *fil* and *clv1* single mutants show some floral meristem initiation defects, with occasional empty cauline leaves or filamentous structures. The *lfy* mutation greatly enhances the *fil* and *clv1* floral defects. In double mutant plants, most floral primordia are replaced by empty cauline leaves or filaments, which are determinate structures lacking meristematic potential (Sawa *et al.*, 1999a). *PINOID* (*PID*) is another regulator (from the auxin signaling cascade) that contributes to meristem development (Bennett *et al.*, 1995; Christensen *et al.*, 2000). *pid* floral meristem defects are also strongly enhanced in the *pid lfy* double mutant even under growth conditions where the *pid* single mutant only displays a very mild phenotype (Ezhova *et al.*, 2000). Another striking example comes from analysis of *BOP* genes (Norberg *et al.*, 2005): empty cauline leaves replace some flowers in the *bop1 bop2 lfy* triple mutant but not in the *bop1 bop2* double mutant. Thus, LFY does stimulate floral meristem outgrowth, but this role is masked by redundant pathways.

Ectopic expression of *LFY* at a time when these pathways are less active revealed the importance of *RAX1*

induction by LFY for precocious emergence of meristems in the axils of rosette leaves. There is evidence that this induction also occurs in flowers: (i) *RAX1* mRNA is present in early stage 1 flower meristems just after LFY expression starts (Keller *et al.*, 2006; Muller *et al.*, 2006), (ii) LFY strongly binds the *RAX1* locus at three locations in inflorescence tissues (Winter *et al.*, 2011), and (iii) expression of LFY-VP16 induces *RAX1* expression in inflorescences (Figure 4a). However, expression of *RAX1* is not lower in the single *lfy* mutant, probably because it is also induced by other regulators such as the *LATERAL ORGAN FUSION* (*LOF*) genes (Lee *et al.*, 2009). Similarly, the single *rax1* mutation does not affect development of flowers but only suppresses some axillary meristems at the base of leaves from plants grown under short-day conditions. Genes such as *LATERAL SUPPRESSOR* (*LAS*) (Greb *et al.*, 2003) and *REGULATOR OF AXILLARY MERISTEM FORMATION* (*ROX*) (Yang *et al.*, 2012) have been shown to act in parallel with *RAX1* to stimulate meristem growth. Interestingly, these two genes are required for axillary meristem emergence but not for flowers, although they are both expressed in floral primordia: they are thus prominent candidates to act redundantly with *LFY* during the reproductive phase.

Down-regulation of *ARR7* expression by LFY (as indicated by analysis of the *lfy-12* mutant) may also contribute to meristem emergence. *ARR7* is a negative regulator of cytokinin signaling (Lee *et al.*, 2007). Cytokinin is a phytohormone that is known to promote axillary meristem growth (Tantikanjana *et al.*, 2001) and is directly repressed by WUS during early flower development (Leibfried *et al.*, 2005). As LFY and WUS interact to induce *AG* expression (Lohmann *et al.*, 2001), it is possible that they also collaborate to repress *ARR7*. A direct interaction between LFY and the *ARR7* promoter was observed both *in vitro* (Leibfried *et al.*, 2005) and *in vivo* in seedlings ectopically expressing LFY (Moyroud *et al.*, 2011; Winter *et al.*, 2011). In addition to the cytokinin pathway, auxin signaling may also be important downstream of LFY: several genes from the auxin pathway are bound by LFY in ChIP experiments (Moyroud *et al.*, 2011; Winter *et al.*, 2011), and LAS has been shown to act upstream of auxin components (Greb *et al.*, 2003). Meristem emergence may thus result from both convergence of LFY and LAS action on hormones and stimulation of the RAX1 pathway.

AP1 and LFY share the floral function, but only LFY stimulates meristem development

We observed that constitutive *AP1* expression only mildly affects meristem development compared to *LFY*. The fact that *AP1* does not participate in meristem outgrowth is supported by the phenotypes of double mutants such as *ap1 clv1*, *ap1 fil* or *ap1 bop1 bop2* that do not display the empty cauline leaves or filamentous structures observed in double or triple mutants that include the *lfy* mutation (Clark *et al.*, 1996; Chen *et al.*, 1999; Xu *et al.*, 2010). This may seem surprising given that LFY and AP1 share many floral functions and bind to a common set of target genes, including the *RAX1* locus (Figure 4). However, the fact that *RAX1* is not induced but instead is repressed by AP1 (Kaufmann *et al.*, 2010) provides a striking explanation for the differential effect of these two floral meristem identity genes on meristem stimulation: AP1 probably contributes to the loss of meristematic character of the floral meristem established by LFY.

A developmental scenario for meristem emergence and floral fate determination

The data provided here and elsewhere suggests the following sequence of events for early flower development (Figure 5). The site of leaf or flower meristem emergence is determined by the auxin maximum (Kuhlemeier, 2007; Vernoux *et al.*, 2010). After the floral transition, auxin accumulation stimulates *LFY* expression in the floral anlage (stage 0). LFY contributes to outgrowth of the meristem and expression of meristematic genes such as *WUS*, *CLV3* and *UFO* by inducing *RAX1* and probably repressing *ARR7* together with WUS. Together with some of its own targets such as AP1 or LMI1 (Saddic *et al.*, 2006), LFY also confers floral fate to the nascent meristem (stage 2). Acquisition of floral identity involves the induction of floral homeotic genes as well as loss of inflorescence meristem genes through repression of *RAX1*, *SUPPRESSOR OF OVEREXPRESSION OF CONSTANS1* (*SOC1*), *AGAMOUS-LIKE24* (*AGL24*) and *SHORT VEGETATIVE PHASE* (*SVP*) by AP1 (Liu *et al.*, 2007; Kaufmann *et al.*, 2010) and of *WUS* by AG (Lohmann *et al.*, 2001). This scenario provides another

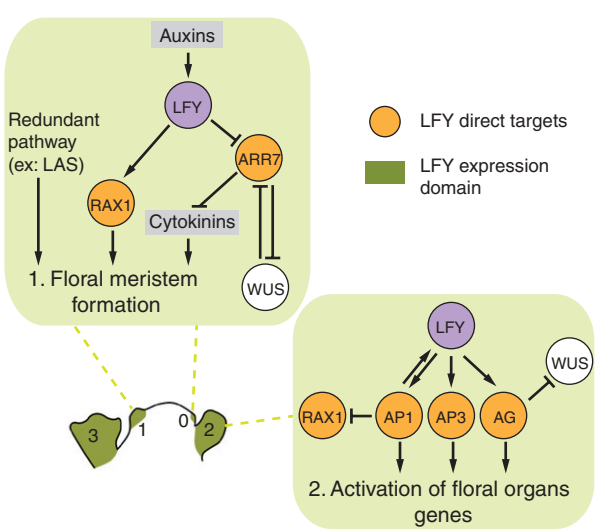

Figure 5. Speculative model in which the links between *LFY*, *RAX1* and *ARR7* are placed in the context of flower meristem development and integrated with other known regulation pathways. The numbers on the inflorescence section indicate floral stages.

illustration of the importance of the timing of these feed-forward loops for proper development of the flower. Controlling both the emergence of the meristem and its floral determination by the same regulator (LFY) may be an efficient way to couple both events and ensure they do not occur independently, when environmental conditions affect the cell division rate for example. Firm demonstration of the role of the LFY-RAX1 module in flowers will require further investigation in genetic contexts with reduced redundancy between pathways.

The action of LFY on meristems explains the *lfy* phenotypes in various plants

Homologs of *LFY* are found in all angiosperms, but the phenotypes of *lfy* loss-of-function mutants differ in some species. Moyroud *et al.* (2009, 2010) proposed that a meristematic function of *LFY* provides a common explanation for the phenotypes observed in various species, such as the reduced number of flowers and tillers of the *rice floricaula leafy* (*rfl*) mutant (Kyozuka *et al.*, 1998; Rao *et al.*, 2008; Ikeda-Kawakatsu *et al.*, 2012) or simple leaf development when the *LFY* ortholog is mutated in pea (*Pisum sativum*) or *Medicago truncatula* (Hofer *et al.*, 1997; Champagne *et al.*, 2007; Wang *et al.*, 2008). It will be interesting to determine whether the molecular mechanism unraveled in Arabidopsis is shared by other species, and whether homologs of *RAX1* contribute to rice tiller or inflorescence development or to leaf dissection in some legumes. In tomato, two *RAX1* co-orthologs, named *BLIND* (*BL*) and *POTATO LEAF* (*C*), control shoot architecture and leaf development (Schmitz *et al.*, 2002; Busch *et al.*, 2011). Mutations of these genes reduce plant branching and leaf complexity. Interestingly, mutations in *FALSIFLORA* (*FA*), the *LFY* ortholog in tomato (*Solanum lycopersicum*), also affect both processes (Molinero-Rosales *et al.*, 1999). These common phenotypes, together with the overlapping expression patterns of *FA* and *BL*/*C*, are consistent with possible regulation of *BL*/*C* genes by FA in tomato. In the moss *Physcomitrella patens*, LFY homologs were shown to act in the first cell division after fertilization (Tanahashi *et al.*, 2005). It is therefore possible that the ancestral function of LFY was to control of cell division, and that LFY specialized in the emergence of meristems before being co-opted to confer floral fate to the meristems it produced.

EXPERIMENTAL PROCEDURES

Plant material and growth conditions

The *Pro35S:AP1* seeds were a gift from Detlef Weigel (Max Planck Institute, Tübingen, Germany). The *ProCLV3:GUS* line (Brand *et al.*, 2002) and the *rax1-3* mutant T-DNA line (SALK_071748) (Muller *et al.*, 2006) were obtained from the Nottingham Arabidopsis Stock Centre (http://arabidopsis.info). All mutants and transgenic lines used are in the *A. thaliana* Columbia-0 accession.

Seeds were sown on soil or surface-sterilized and grown in Petri dishes on Murashige and Skoog basal salt mixture medium (Sigma-Aldrich, www.sigmaaldrich.com). Plants were transferred to soil and grown at 22°C under long-day conditions (16 h of 100 μE light) or short-day conditions (8 h of 100 μE light). The *ProLFY:LFY-VP16* plants have been described previously (Parcy *et al.*, 1998).

Plant genotyping

Plants carrying the *lfy-12* mutation were genotyped using the end-point genotyping program with a Light Cycler 480 (Roche, http://www.roche.com) as described by Benlloch *et al.* (2011) or using the following dCAPS primers: forward (5′-TCAAGCACCACCTCC GGTTCCACCTCCA-3′) and reverse (5′-CGGACGAAAACCCTACGCT GAACCACCA-3′). Only the wild-type 85 bp PCR product is cleaved by the *Fnu*4HI restriction enzyme. The *RAX1* locus was identified by PCR using primers oHC150 (5′-TGTGAAAAGACCAACCTCACC-3′) and oHC151 (5′-TCGGACATTTCAGTTTGGAAG-3′) for *RAX1*, and the *rax1-3* allele was identified using primers oHC150 and oHC152 (5′-ATTTTGCCGATTTCGGAAC-3′).

Plant vectors and transformation

The pFP100 binary vector (Bensmihen *et al.*, 2004), which contains the *ProAt2S3:GFP in planta* selection marker, was used as a backbone for the following binary constructs: *ProLFY:LFY* (pETH29), *ProLFY:LFY*$_{HARA}$ (pETH39), *Pro35S:LFY* (pCA26) and *Pro35S:LFY*$_{HARA}$ (pSP3). Details of the cloning procedures can be provided upon request. *Agrobacterium tumefaciens* C58 pMP90 was used for stable transformation of wild-type or *lfy-12* heterozygous plants.

Yeast vectors and one-hybrid assay

For yeast experiments, the p424 vector with the *GAL1* promoter was used to clone *LFY*$_{HA}$-*VP16* (pETH32), *LFY*$_{RA}$-*VP16* (pETH46) and *LFY*$_{HARA}$-*VP16* (pETH31) fusions either by conventional cloning or by using the megaprimer strategy (Kirsch and Joly, 1998). Yeast vectors containing *LFY* and *LFY:VP16* (pFP13 and pFP14, respectively) and the *AGAMOUS:LACZ* reporter construct (pFP50) have been described previously (Parcy *et al.*, 1998; Lohmann *et al.*, 2001). Detailed maps for all constructs are available on request. For one-hybrid experiments, effectors (pFP13, pFP14, pETH31, pETH32 or pETH46) and reporter plasmids (pFP50) were co-transformed into *Saccharomyces cerevisiae* strain EGY48 (Invitrogen, www.lifetechnologies.com). β-galactosidase measurements were performed as described previously (Lohmann *et al.*, 2001), except that they were adapted to the Safire2 microplate reader (Tecan, www.tecan.com).

Expression and purification of recombinant LFY proteins

The pET-30a vector (Novagen, www.merckmillipore.com) was used to clone recombinant near full-length LFY [LFY(Δ40), pETH79], LFY$_{HARA}$(Δ40) (pETH156) and LFY$_{HARAKARA}$(Δ40) (pETH180). Because it greatly facilitated expression and purification of these LFY recombinant proteins, the non-conserved first 39 amino acids were omitted in these constructs. The proteins were expressed in the *Escherichia coli* Rosetta™2 (DE3) strain (Novagen, http://www.emdmillipore.com/), and purified on Ni Sepharose™ high-performance resin (GE Healthcare, www.gehealthcare.com) as described in Methods S1.

EMSA experiments

Electrophoretic mobility shift assay were performed as previously described (Moyroud *et al.*, 2011). AP1 oligonucleotides (5′-

GTTGGGGAAGGACCAGTGGTCCGTACAATGT-3′ and 5′-ACATTGT ACGGACCACTGGTCCTTCCCCAA-3′) labeled with the Cy5 fluorophore were prepared as described by Moyroud *et al.* (2011). The binding reactions were performed over 15 min using 100, 500 or 1500 nM LFY in 20 μl binding buffer (10 mM HEPES, 1 mM spermidine, 14 mM EDTA, 30 μg BSA, 0.25% CHAPS, 3% glycerol, 3 mM tris(2-carboxyethyl)phosphine (TCEP), pH 8, and 28 ng/ml fish sperm DNA), and loaded on a native gel (6% acrylamide, 0.5 × TBE). Gels were electrophoresed at 90 V for 70 min at 4°C, and scanned on the Typhoon 9400 scanner (Amersham Biosciences, www.gehealthcare.com).

Systematic evolution of ligands by exponential enrichment experiments

Systematic evolution of ligands by exponential enrichment experiments were performed using fluorescent 73-mers and LFY (Δ40) or LFY_{HARA}(Δ40) proteins. Initially, a random library was synthesized using 73-mers 5′-TGGAGAAGAGGAGAGATCTAGC $(N)_{30}$CTTGTTCTTCTTCGATTCCGG-3′ as template with a fluorescent TAMRA-labelled forward primer (SElex-F, 5′-TGGAGAAGAG GAGAG ATCTAG-3′) and a non-labeled reverse primer (SElex-R, 5′-CCGG AATCGAAGAAGAACAA-3′), as previously described (Moyroud *et al.*, 2011).

For each selection cycle, 1 μM protein was mixed with 10 nM fluorescent dsDNA in 225 μl Selex buffer (20 mM Tris pH 8, 250 mM NaCl, 2 mM $MgCl_2$, 5 mM TCEP, 60 μg/ml fish sperm DNA and 1% glycerol). After a 15 min incubation, 25 μl Ni-NTA magnetic beads (Qiagen, www.qiagen.com), previously equilibrated in Selex buffer, were added to the reaction mix to immobilize DNA/protein complexes via the His tag of the protein. After 30 min incubation, the reaction mix was placed on a tube magnet for 1 min, and the supernatant was removed from the separated beads to eliminate the unbound DNA. Five washes were subsequently performed at 4°C, each of them consisting of adding 250 μl Selex buffer containing 20 μg/ml fish sperm DNA, followed by 2 min incubation and 1 min on the tube magnet to discard the supernatant. Finally, the magnetic beads were resuspended in 50 μl Selex buffer without fish sperm DNA. Selected 73-mers were amplified by PCR as described previously (Moyroud *et al.*, 2011) using 1 μl of the magnetic beads solution as template. PCR products were quantified as previously described (Moyroud *et al.*, 2011), and the selection cycle was repeated three times, each time using the newly synthesized fluorescent DNA as a library. The 73-mers libraries obtained after four cycles of selection were subsequently used for barcoding and high-throughput sequencing.

Barcoding for Illumina sequencing of the SELEX libraries

Oligonucleotides allowing hybridization with the sequencing primer fused to a 6 bp barcode (one unique barcode per library) were added by PCR (PCR#1) to 73-mers of each library selected, using Phusion® DNA polymerase (Ozyme, http://www.ozyme.fr) and 0.5–2 μl of the magnetic beads solution as template, extending the 73-mers into 146 bp dsDNA. Three PCR cycles (PCR#2) were subsequently performed, using 5 μl of PCR#1 product as template, Phusion® DNA polymerase (Ozyme, http://www.ozyme.fr) and Illumina oligonucleotides (http://www.illumina.com/), allowing fixation of the dsDNA to the Illumina sequencing chip. PCR products from PCR#2 (171 bp) were purified using a NucleoSpin Extract II kit (Macherey-Nagel, http://www.mn-net.com), and sequenced on an Illumina platform at the Max Planck Institute for Developmental Biology, Tübingen, Germany.

The 2000 unique most frequent sequences were aligned using MEME software version 4.3.0 (Bailey and Elkan, 1994) using default parameters and imposing symmetry to construct the LFY (Δ40) and the LFY_{HARA}(Δ40) matrix.

Gene expression analysis

RNA extractions were prepared from 50 mg plant tissues using and RNeasy plant RNA extraction kit (Qiagen). Extractions were obtained from 21-day-old seedlings (Col-0 and *Pro35S:LFY* plants cultivated under short-day conditions) or young apices from which older flowers were removed (Col-0, *lfy-12* and *ProLFY:LFY-VP16* plants cultivated under long-day conditions). Total RNAs were treated with Ambion® turbo DNA-free™ DNase (Invitrogen) to reduce genomic DNA contamination. Reverse transcription was performed using MMLV reverse transcriptase (Sigma-Aldrich) from 1 μg of total RNA.

Primers used for real-time PCR were designed using QUANTPRIME software (www.quantprime.de/) and are listed in Table S4. PCR reactions were performed in a 15 μl final volume using 0.1 μM for each primer, 1 × mix SYBR Green JumpStart® (Sigma-Aldrich) and 3.125 ng cDNA in a Rotor Gene 3000 (Qiagen) with default cycle parameters. The relative expression of a target gene was calculated by the $\Delta\Delta C_t$ method as described by Pfaffl (2001) using the reference gene At2g28390 as previously described (Czechowski *et al.*, 2005; Guenin *et al.*, 2009). Statistical analyses were performed using REST 2009 software (Pfaffl *et al.*, 2002).

Decapitation experiment

Plants were grown for 1 month under short-day conditions and then transferred to long-day conditions. The primary inflorescence was cut once it reached 10–15 cm, i.e. after 20 days for $Pro35S:LFY_{HARA}$ or 26 days for wild-type and *lfy-12* plants. The number of secondary inflorescences was scored on the day of decapitation and 10 days later. Parametric statistics for the percentage of rosette leaves bearing a shoot or flower were applied after arcsine root transformation; 95% confidence intervals were found with the usual *t* distribution and then back-transformed to percentages.

Histology

Tissues were fixed in formaldehyde/acetic acid/ethanol (FAA), and infiltration with paraffin was performed in an ASP300 embedding automat (Leica, http://www.leica.com). Thin sections (9–12 μm) were prepared on an EG1160 microtome (Leica) and transferred to glass slides. Staining was performed with toluidine blue. Images were taken on an Axioplan2 (Zeiss, www.zeiss.com) equipped with an AxioCam HRc digital camera (Zeiss). GUS staining was performed as described previously (Parcy *et al.*, 1998).

Model describing the appearance of the axillary meristem staining

We assumed that the probability of a plant having entered the phase of meristematic development (production of axillary meristem at the axil of rosette leaves) was a sigmoid function of time, characterized by its mean d_{switch} and its temporal uncertainty τ; thus this probability on day d was modeled as $P(\text{meristematic} \mid d) = \sigma((d - d_{switch})/\tau)$, where σ is the logistic function: $\sigma(x) = 1/[1 + \exp(-x)]$. In the meristematic development phase, we assumed that a Poisson process of rate λ governed the appearance of meristems: thus the probability of observing n meristems t days after the switch to the meristematic phase is $\pi(n, \lambda, t) = (\lambda t)^n/n! \exp(-\lambda t)$; before this meristematic phase, *P*

($n = 0$) = 1. With these assumptions, the overall probability of observing $n > 0$ meristems on day d is

$$p(n|d) = 1/\tau \int_0^d \sigma' \left[\frac{t - d_{switch}}{\tau}\right] \pi(n, \lambda, d - t)\mathrm{d}t$$

By maximizing the likelihood of the experimental meristem counts in this model, we derived the parameters d_{switch}, τ and λ for each strain. Likelihood ratio tests were then used to test the statistical significance of the parameter differences across strains. As τ and λ were not significantly different across strains ($P > 0.1$ for both), the model illustrated on Figure 3(a) was constrained to use a single value for each of these two parameters, with three values of d_{switch} (one for each strain).

ACKNOWLEDGEMENTS

We thank R. Dumas, R. Benlloch (UPSC, Umeå, Sweden), O. Nilsson (UPSC, Umeå, Sweden), A. Mathelier (CMMT, Vancouver, Canada), W. Wasserman (CMMT, Vancouver, Canada), P. Baraduc (CNC, Lyon, France) and M. Nanao (EMBL, Grenoble, France) for help with experiment or data analysis, D. Weigel (MPI, Tuebingen, Germany) and N. Warthman (MPI, Tuebingen, Germany) for SELEX sequencing, P. Cubas (CNB, Madrid, Spain) and P. Doerner for discussion, and V. Pautot (INRA, Versailles, France), L. Yan (Dept. of Organismic and Evolutionary Biology Harvard University, USA) and P. Laufs (INRA, Versailles, France) for critical reading of the manuscript. This work is supported by grants from the Charmful ANR (Agence Nationale de la Recherche) program and by the Natural Sciences and Engineering Research Council of Canada to V.G.

SUPPORTING INFORMATION

Additional Supporting Information may be found in the online version of this article.

Method S1. Expression and purification of LFY proteins from bacteria.

Figure S1. Inflorescence phenotype of *ProLFY:LFY lfy-12* and *ProLFY:LFY$_{HARA}$ lfy-12* plants.

Figure S2. Production rate of rosette leaves in *Pro35S:LFY* and *Pro35S:AP1* plants.

Figure S3. Structures developing at the axils of cotyledons of *Pro35S:LFY* and *Pro35S:LFY$_{HARA}$* plants.

Table S1. Floral phenotype of *lfy-12* plant complemented by *LFY* or *LFY$_{HARA}$* cDNA.

Table S2. Distribution of phenotypic classes among *Pro35S:LFY* and *Pro35S:LFY$_{HARA}$* T_1 plants.

Table S3. *CLV3:GUS* activity in axillary meristems of *Pro35S:LFY* seedlings.

Table S4. Oligonucleotides used for the quantitative PCR experiments.

REFERENCES

Aguilar-Martinez, J.A., Poza-Carrion, C. and Cubas, P. (2007) Arabidopsis BRANCHED1 acts as an integrator of branching signals within axillary buds. *Plant Cell*, **19**, 458–472.

Anderson, G.H., Alvarez, N.D., Gilman, C., Jeffares, D.C., Trainor, V.C., Hanson, M.R. and Veit, B. (2004) Diversification of genes encoding *mei2*-like RNA binding proteins in plants. *Plant Mol. Biol.* **54**, 653–670.

Bailey, T.L. and Elkan, C. (1994) Fitting a mixture model by expectation maximization to discover motifs in biopolymers. *Proc. Int. Conf. Intell. Syst. Mol. Biol.* **2**, 28–36.

Benlloch, R., Kim, M.C., Sayou, C., Thevenon, E., Parcy, F. and Nilsson, O. (2011) Integrating long-day flowering signals: a LEAFY binding site is essential for proper photoperiodic activation of APETALA1. *Plant J.* **67**, 1094–1102.

Bennett, S.R.M., Alavrez, J., Bossinegr, G. and Smyth, D.R. (1995) Morphogenesis in *pinoid* mutants of *Arabidopsis thaliana*. *Plant J.* **8**, 505–520.

Bensmihen, S., To, A., Lambert, G., Kroj, T., Giraudat, J. and Parcy, F. (2004) Analysis of an activated *ABI5* allele using a new selection method for transgenic Arabidopsis seeds. *FEBS Lett.* **561**, 127–131.

Blazquez, M.A., Ferrandiz, C., Madueno, F. and Parcy, F. (2006) How floral meristems are built. *Plant Mol. Biol.* **60**, 855–870.

Brand, U., Grunewald, M., Hobe, M. and Simon, R. (2002) Regulation of CLV3 expression by two homeobox genes in Arabidopsis. *Plant Physiol.* **129**, 565–575.

Busch, B.L., Schmitz, G., Rossmann, S., Piron, F., Ding, J., Bendahmane, A. and Theres, K. (2011) Shoot branching and leaf dissection in tomato are regulated by homologous gene modules. *Plant Cell*, **23**, 3595–3609.

Champagne, C.E., Goliber, T.E., Wojciechowski, M.F., Mei, R.W., Townsley, B.T., Wang, K., Paz, M.M., Geeta, R. and Sinha, N.R. (2007) Compound leaf development and evolution in the legumes. *Plant Cell*, **19**, 3369–3378.

Chen, Q., Atkinson, A., Otsuga, D., Christensen, T., Reynolds, L. and Drews, G.N. (1999) The Arabidopsis *FILAMENTOUS FLOWER* gene is required for flower formation. *Development*, **126**, 2715–2726.

Christensen, S.K., Dagenais, N., Chory, J. and Weigel, D. (2000) Regulation of auxin response by the protein kinase PINOID. *Cell*, **100**, 469–478.

Clark, S.E., Running, M.P. and Meyerowitz, E.M. (1993) CLAVATA1, a regulator of meristem and flower development in Arabidopsis. *Development*, **119**, 397–418.

Clark, S.E., Jacobsen, S.E., Levin, J.Z. and Meyerowitz, E.M. (1996) The *CLAVATA* and *SHOOT MERISTEMLESS* loci competitively regulate meristem activity in *Arabidopsis*. *Development*, **122**, 1567–1575.

Czechowski, T., Stitt, M., Altmann, T., Udvardi, M.K. and Scheible, W.R. (2005) Genome-wide identification and testing of superior reference genes for transcript normalization in Arabidopsis. *Plant Physiol.* **139**, 5–17.

Ezhova, T.A., Soldatova, O.P., Kalinina, A. and Medvedev, S.S. (2000) Interaction of ABRUPTUS/PINOID and LEAFY genes during floral morphogenesis in *Arabidopsis thaliana* (L.) Heynh. *Genetika*, **36**, 1682–1687 (in Russian).

Fornara, F., de Montaigu, A. and Coupland, G. (2010) SnapShot: control of flowering in Arabidopsis. *Cell*, **141**, 550, 550.e2

Greb, T., Clarenz, O., Schafer, E., Muller, D., Herrero, R., Schmitz, G. and Theres, K. (2003) Molecular analysis of the *LATERAL SUPPRESSOR* gene in Arabidopsis reveals a conserved control mechanism for axillary meristem formation. *Genes Dev.* **17**, 1175–1187.

Guenin, S., Mauriat, M., Pelloux, J., Van Wuytswinkel, O., Bellini, C. and Gutierrez, L. (2009) Normalization of qRT-PCR data: the necessity of adopting a systematic, experimental conditions-specific, validation of references. *J. Exp. Bot.* **60**, 487–493.

Hamès, C., Ptchelkine, D., Grimm, C., Thevenon, E., Moyroud, E., Gerard, F., Martiel, J.L., Benlloch, R., Parcy, F. and Muller, C.W. (2008) Structural basis for LEAFY floral switch function and similarity with helix-turn-helix proteins. *EMBO J.* **27**, 2628–2637.

Hofer, J., Turner, L., Hellens, R., Ambrose, M., Matthews, P., Michael, A. and Ellis, N. (1997) *UNIFOLIATA* regulates leaf and flower morphogenesis in pea. *Curr. Biol.* **7**, 581–587.

Horiguchi, G., Kim, G.T. and Tsukaya, H. (2005) The transcription factor AtGRF5 and the transcription coactivator AN3 regulate cell proliferation in leaf primordia of *Arabidopsis thaliana*. *Plant J.* **43**, 68–78.

Ikeda-Kawakatsu, K., Maekawa, M., Izawa, T., Itoh, J. and Nagato, Y. (2012) *ABERRANT PANICLE ORGANIZATION 2/RFL*, the rice ortholog of Arabidopsis *LEAFY*, suppresses the transition from inflorescence meristem to floral meristem through interaction with *APO1*. *Plant J.* **69**, 168–180.

Irish, V.F. (2010) The flowering of Arabidopsis flower development. *Plant J.* **61**, 1014–1028.

Kaufmann, K., Wellmer, F., Muino, J.M. *et al.* (2010) Orchestration of floral initiation by APETALA1. *Science*, **328**, 85–89.

Keller, T., Abbott, J., Moritz, T. and Doerner, P. (2006) Arabidopsis REGULATOR OF AXILLARY MERISTEMS1 controls a leaf axil stem cell niche and modulates vegetative development. *Plant Cell*, **18**, 598–611.

Kim, J.H., Choi, D. and Kende, H. (2003) The AtGRF family of putative transcription factors is involved in leaf and cotyledon growth in Arabidopsis. *Plant J.* **36**, 94–104.

Kirsch, R.D. and Joly, E. (1998) An improved PCR-mutagenesis strategy for two-site mutagenesis or sequence swapping between related genes. *Nucleic Acids Res.* **26**, 1848–1850.

Kuhlemeier, C. (2007) Phyllotaxis. *Trends Plant Sci.* **12**, 143–150.
Kyozuka, J., Konishi, S., Nemoto, K., Izawa, T. and Shimamoto, K. (1998) Down-regulation of RFL, the FLO/LFY homolog of rice, accompanied with panicle branch initiation. *Proc. Natl Acad. Sci. USA*, **95**, 1979–1982.
Lebedeva, O.V., Ondar, U.N., Penin, A.A. and Ezhova, T.A. (2005) Effect of the *ABRUPTUS*/*PINOID* gene on expression of the *LEAFY* gene in *Arabidopsis thaliana*. *Genetika*, **41**, 559–565 (in Russian).
Lee, D.J., Park, J.Y., Ku, S.J., Ha, Y.M., Kim, S., Kim, M.D., Oh, M.H. and Kim, J. (2007) Genome-wide expression profiling of *ARABIDOPSIS RESPONSE REGULATOR 7* (*ARR7*) overexpression in cytokinin response. *Mol. Genet. Genomics*, **277**, 115–137.
Lee, D.K., Geisler, M. and Springer, P.S. (2009) LATERAL ORGAN FUSION1 and LATERAL ORGAN FUSION2 function in lateral organ separation and axillary meristem formation in Arabidopsis. *Development*, **136**, 2423–2432.
Leibfried, A., To, J.P., Busch, W., Stehling, S., Kehle, A., Demar, M., Kieber, J.J. and Lohmann, J.U. (2005) WUSCHEL controls meristem function by direct regulation of cytokinin-inducible response regulators. *Nature*, **438**, 1172–1175.
Levin, J.Z., Fletcher, J.C., Chen, X. and Meyerowitz, E.M. (1998) A genetic screen for modifiers of UFO meristem activity identifies three novel *FUSED FLORAL ORGANS* genes required for early flower development in Arabidopsis. *Genetics*, **149**, 579–595.
Liu, C., Zhou, J., Bracha-Drori, K., Yalovsky, S., Ito, T. and Yu, H. (2007) Specification of Arabidopsis floral meristem identity by repression of flowering time genes. *Development*, **134**, 1901–1910.
Liu, C., Thong, Z. and Yu, H. (2009) Coming into bloom: the specification of floral meristems. *Development*, **136**, 3379–3391.
Lohmann, J.U., Hong, R.L., Hobe, M., Busch, M.A., Parcy, F., Simon, R. and Weigel, D. (2001) A molecular link between stem cell regulation and floral patterning in Arabidopsis. *Cell*, **105**, 793–803.
Mandel, M.A. and Yanofsky, M.F. (1995) A gene triggering flower formation in Arabidopsis. *Nature*, **377**, 522–524.
Molinero-Rosales, N., Jamilena, M., Zurita, S., Gomez, P., Capel, J. and Lozano, R. (1999) *FALSIFLORA*, the tomato orthologue of *FLORICAULA* and *LEAFY*, controls flowering time and floral meristem identity. *Plant J.* **20**, 685–693.
Moyroud, E., Tichtinsky, G. and Parcy, F. (2009) The LEAFY floral regulators in angiosperms: conserved proteins with diverse roles. *J. Plant Biol.* **52**, 177–185.
Moyroud, E., Kusters, E., Monniaux, M., Koes, R. and Parcy, F. (2010) LEAFY blossoms. *Trends Plant Sci.* **15**, 346–352.
Moyroud, E., Minguet, E.G., Ott, F. *et al.* (2011) Prediction of regulatory interactions from genome sequences using a biophysical model for the Arabidopsis LEAFY transcription factor. *Plant Cell*, **23**, 1293–1306.
Muller, D., Schmitz, G. and Theres, K. (2006) Blind homologous R2R3 Myb genes control the pattern of lateral meristem initiation in Arabidopsis. *Plant Cell*, **18**, 586–597.
Nicol, J.W., Helt, G.A., Blanchard, S.G. Jr, Raja, A. and Loraine, A.E. (2009) The Integrated Genome Browser: free software for distribution and exploration of genome-scale datasets. *Bioinformatics*, **25**, 2730–2731.
Norberg, M., Holmlund, M. and Nilsson, O. (2005) The *BLADE ON PETIOLE* genes act redundantly to control the growth and development of lateral organs. *Development*, **132**, 2203–2213.
Parcy, F., Nilsson, O., Busch, M.A., Lee, I. and Weigel, D. (1998) A genetic framework for floral patterning. *Nature*, **395**, 561–566.
Parcy, F., Bomblies, K. and Weigel, D. (2002) Interaction of *LEAFY*, *AGAMOUS* and *TERMINAL FLOWER1* in maintaining floral meristem identity in *Arabidopsis*. *Development*, **129**, 2519–2527.
Pfaffl, M.W. (2001) A new mathematical model for relative quantification in real-time RT-PCR. *Nucleic Acids Res.* **29**, e45.
Pfaffl, M.W., Horgan, G.W. and Dempfle, L. (2002) Relative expression software tool (REST) for group-wise comparison and statistical analysis of relative expression results in real-time PCR. *Nucleic Acids Res.* **30**, e36.
Pose, D., Yant, L. and Schmid, M. (2012) The end of innocence: flowering networks explode in complexity. *Curr. Opin. Plant Biol.* **15**, 45–50.
Rao, N.N., Prasad, K., Kumar, P.R. and Vijayraghavan, U. (2008) Distinct regulatory role for RFL, the rice LFY homolog, in determining flowering time and plant architecture. *Proc. Natl Acad. Sci. USA*, **105**, 3646–3651.
Ratcliffe, O.J., Bradley, D.J. and Coen, E.S. (1999) Separation of shoot and floral identity in Arabidopsis. *Development*, **126**, 1109–1120.
Ruiz-Garcia, L., Madueno, F., Wilkinson, M., Haughn, G., Salinas, J. and Martinez-Zapater, J.M. (1997) Different roles of flowering-time genes in the activation of floral initiation genes in Arabidopsis. *Plant Cell*, **9**, 1921–1934.
Running, M.P., Fletcher, J.C. and Meyerowitz, E.M. (1998) The *WIGGUM* gene is required for proper regulation of floral meristem size in Arabidopsis. *Development*, **125**, 2545–2553.
Saddic, L.A., Huvermann, B., Bezhani, S., Su, Y., Winter, C.M., Kwon, C.S., Collum, R.P. and Wagner, D. (2006) The LEAFY target LMI1 is a meristem identity regulator and acts together with LEAFY to regulate expression of *CAULIFLOWER*. *Development*, **133**, 1673–1682.
Sawa, S., Ito, T., Shimura, Y. and Okada, K. (1999a) FILAMENTOUS FLOWER controls the formation and development of Arabidopsis inflorescences and floral meristems. *Plant Cell*, **11**, 69–86.
Sawa, S., Watanabe, K., Goto, K., Liu, Y.G., Shibata, D., Kanaya, E., Morita, E.H. and Okada, K. (1999b) *FILAMENTOUS FLOWER*, a meristem and organ identity gene of Arabidopsis, encodes a protein with a zinc finger and HMG-related domains. *Genes Dev.* **13**, 1079–1088.
Schmitz, G., Tillmann, E., Carriero, F., Fiore, C., Cellini, F. and Theres, K. (2002) The tomato *Blind* gene encodes a MYB transcription factor that controls the formation of lateral meristems. *Proc. Natl Acad. Sci. USA*, **99**, 1064–1069.
Siriwardana, N.S. and Lamb, R.S. (2012) A conserved domain in the N–terminus is important for LEAFY dimerization and function in *Arabidopsis thaliana*. *Plant J.* **71**, 736–749.
Stirnberg, P., van De Sande, K. and Leyser, H.M. (2002) MAX1 and MAX2 control shoot lateral branching in Arabidopsis. *Development*, **129**, 1131–1141.
Tanahashi, T., Sumikawa, N., Kato, M. and Hasebe, M. (2005) Diversification of gene function: homologs of the floral regulator *FLO*/*LFY* control the first zygotic cell division in the moss *Physcomitrella patens*. *Development*, **132**, 1727–1736.
Tantikanjana, T., Yong, J.W., Letham, D.S., Griffith, M., Hussain, M., Ljung, K., Sandberg, G. and Sundaresan, V. (2001) Control of axillary bud initiation and shoot architecture in Arabidopsis through the *SUPERSHOOT* gene. *Genes Dev.* **15**, 1577–1588.
Vernoux, T., Kronenberger, J., Grandjean, O., Laufs, P. and Traas, J. (2000) PIN-FORMED 1 regulates cell fate at the periphery of the shoot apical meristem. *Development*, **127**, 5157–5165.
Vernoux, T., Besnard, F. and Traas, J. (2010) Auxin at the shoot apical meristem. *Cold Spring Harb. Perspect. Biol.* **2**, a001487.
Wagner, D. (2009) Flower morphogenesis: timing is key. *Dev. Cell*, **16**, 621–622.
Wang, H., Chen, J., Wen, J., Tadege, M., Li, G., Liu, Y., Mysore, K.S., Ratet, P. and Chen, R. (2008) Control of compound leaf development by *FLORICAULA*/*LEAFY* ortholog *SINGLE LEAFLET1* in *Medicago truncatula*. *Plant Physiol.* **146**, 1759–1772.
Weigel, D. and Nilsson, O. (1995) A developmental switch sufficient for flower initiation in diverse plants. *Nature*, **377**, 495–500.
Winter, C.M., Austin, R.S., Blanvillain-Baufume, S. *et al.* (2011) LEAFY target genes reveal floral regulatory logic, cis motifs, and a link to biotic stimulus response. *Dev. Cell*, **20**, 430–443.
Xu, M., Hu, T., McKim, S.M., Murmu, J., Haughn, G.W. and Hepworth, S.R. (2010) Arabidopsis BLADE-ON-PETIOLE1 and 2 promote floral meristem fate and determinacy in a previously undefined pathway targeting *APETALA1* and *AGAMOUS-LIKE24*. *Plant J.* **63**, 974–989.
Yalovsky, S., Kulukian, A., Rodriguez-Concepcion, M., Young, C.A. and Gruissem, W. (2000) Functional requirement of plant farnesyltransferase during development in Arabidopsis. *Plant Cell*, **12**, 1267–1278.
Yang, F., Wang, Q., Schmitz, G., Muller, D. and Theres, K. (2012) The bHLH protein ROX acts in concert with RAX1 and LAS to modulate axillary meristem formation in Arabidopsis. *Plant J.* **71**, 61–70.
Zhao, Y., Granas, D. and Stormo, G.D. (2009) Inferring binding energies from selected binding sites. *PLoS Comput. Biol.* **5**, e1000590.

